Semiconductor waveguide inversion in disordered narrow band-gap materials

M. J. Gilbert,[a] R. Akis, and D. K. Ferry
Department of Electrical Engineering and Center for Solid State Electronics Research, Arizona State University, Tempe, Arizona 85287-5706

(Received 20 January 2003; accepted 3 May 2003; published 5 August 2003)

It has been previously demonstrated that it is possible to form the NOT gate in a coupled semiconductor waveguide structure in III–V materials. However, to this point, investigations have assumed the materials to be perfect. In this article, we present results of a semiconductor waveguide inverter in GaAs and InAs with disordered material effects included in the simulation. The behavior of the device clearly shows that with the inclusion of mild to moderate disorder in these materials, waveguide NOT gate function is still possible. Nevertheless, under heavy disorder in the system, clear switching becomes impossible. © *2003 American Vacuum Society.*
[DOI: 10.1116/1.1589521]

Much of quantum computation and information theory has been structured around the use of the qubit.[1] Two or more bits of quantum information are coupled together to achieve basic logic structures for subsequent processing, whereby the most basic and essential coupling of qubits is the controlled not gate (CNOT). Before a CNOT construct can be realized, we must first demonstrate the operation of a NOT gate. It has been shown that, in coupled semiconductor waveguide structures, it is possible to transfer the incident electron density from an input waveguide to an output waveguide using either the application of a magnetic field perpendicular to the direction of density propagation or through the addition of an applied bias across the coupled waveguide structure.[2] While the theoretical operation of the device has been shown to work, the materials in which this device is fabricated have been assumed to be perfect. Here, we investigate whether the semiconductor switching process, in different III–V semiconductor hetrostructures (GaAs and InAs), remains possible in the presence of disorder in the material. We present the results of studies on GaAs- and InAs-based semiconductor waveguide invertors, with attention given to the role of disorder and dissipation.

The structure studied here is shown in Fig. 1. Two parallel waveguides, separated by an electrostatic potential barrier, are coupled via a tunnel region. The input (top) waveguide has a uniform width of 35 nm from start to finish, whereas the output (bottom) waveguide is narrowed at the source end with a width of 25 nm and then widens to a width of 45 nm after the coupling region in the middle of the structure. This wider output region assures that modes propagate through the coupling region and do not decay. The electrostatic potential barrier that separates the input and output waveguides begins with a width of 50 nm and then narrows to 25 nm after the coupling region. To achieve a more realistic potential profile for the barrier, the initial hard wall potential has been smoothed with a Gaussian distribution. The potential barrier, however, is still sufficiently high to prevent any leakage (from the input waveguide to the output waveguide) and assures all transfer of density from the input to the output occurs in the coupling region.

The Fermi energies in the structure are chosen to be 2 and 9 meV corresponding to carrier densities of 5.6×10^{10} and 9×10^{10} cm^{-2} in GaAs and InAs, respectively. These Fermi energies have been chosen so that only one mode is excited in the input waveguide of the structure for a given material. Since the input waveguide structure is wider than the output waveguide, the mode that is excited at this energy will only propagate in the wider input waveguide. The particular dimensions of the waveguide structure can be easily scaled as long as the constraints mentioned are honored. This simulation is performed on a discretized grid using a variation of the Usuki mode matching technique via the scattering matrix,[3] using a grid spacing of 5 nm.

With the Fermi energy in the system defined, in Fig. 2 we now vary the coupling length in the materials. We see the initial state of the qubit is plotted against the coupling length variation for GaAs and InAs. We find that there is a very periodic pattern in the probability density transfer at each respective Fermi energy. In Fig. 2(a), for GaAs we find a period of approximately 300 nm with pure states occurring in intervals of 150 nm. In Fig. 2(b), for InAs, the period appears to be approximately 400 nm whereby we recover the superposition of the states at every 200 nm. Based on the periodicity shown in Fig. 2, we now select coupling lengths which correspond to T_{11} maxima. For GaAs, this coupling length is 335 nm and for InAs the selected coupling length is 400 nm.

In Fig. 3, we plot the results of adding a voltage drop, ranging from 0 to -1.0 mV for GaAs and 0 to -7 mV for InAs, across the coupled waveguide structure with the anode at the right and the cathode at the left of the structure. This adds an extra degree of freedom to the carriers in the system, and it is no longer viable to discuss the operation of the device in terms of just the transmission and reflection of incident modes. The addition of an extra degree of freedom to the carriers excites extra output modes which are indistin-

[a]Author to whom correspondence should be addressed; electronic mail: matthew.gilbert@asu.edu

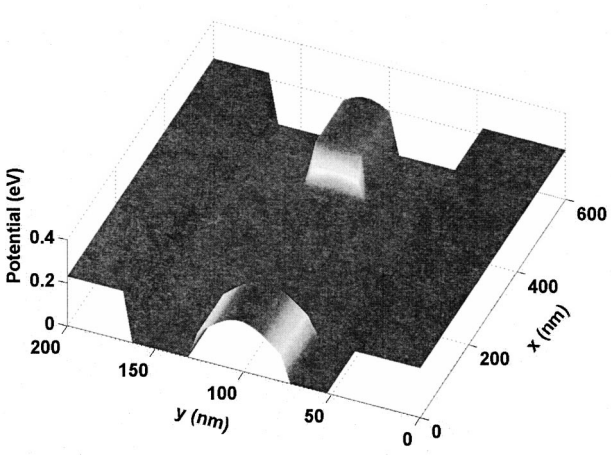

FIG. 1. Plot of the coupled waveguide structure under consideration. In this figure the coupling length between the two waveguides is 335 nm. The right hand side of the structure ($x=600$ nm) is defined to be the anode while the cathode is defined to be the left hand side of the structure ($x=0$ nm).

guishable in the total transmission from the initially excited mode (determined by the setting of the Fermi energy). Therefore, in order to determine the extent to which our device switches from one pure state to the next, we use the Landauer formula[4] to integrate over the individual transmissions

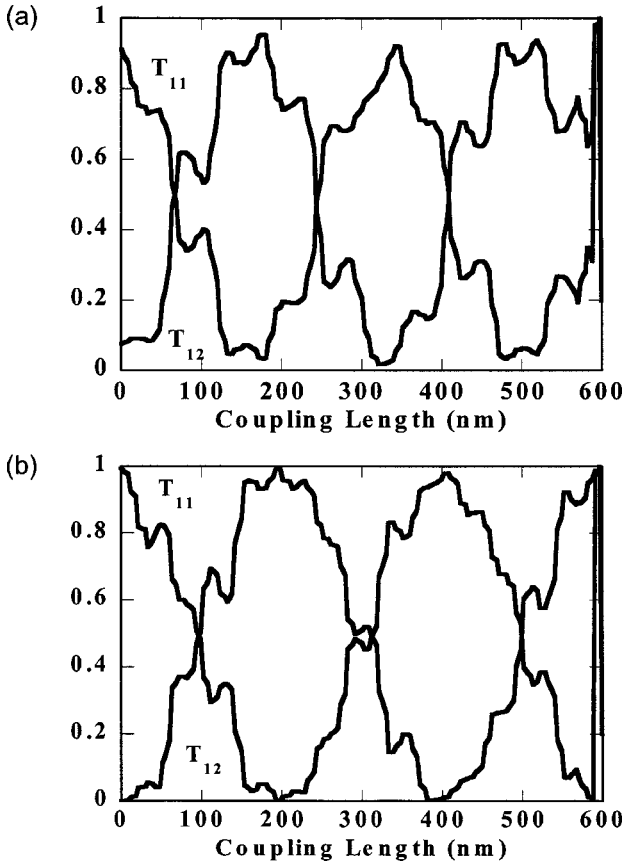

FIG. 2. (a) The individual transmissions (T_{11} and T_{12}) plotted over the coupling length between the two waveguides for GaAs. (b) The individual transmissions (T_{11} and T_{12}) plotted over the coupling length between the two waveguides for InAs.

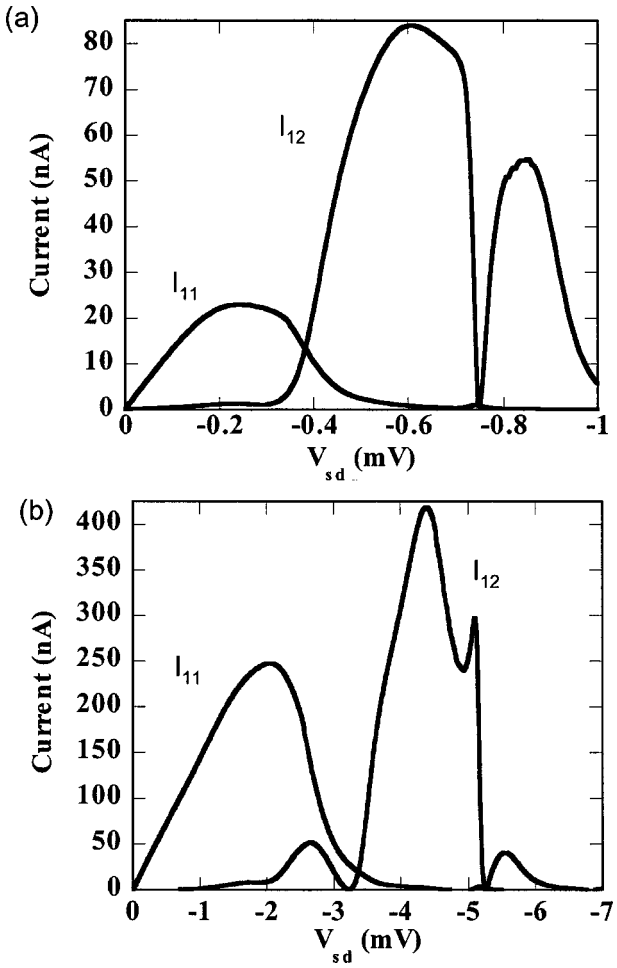

FIG. 3. (a) Output currents I_{11} and I_{12} plotted over an applied source-drain voltage ranging from 0 to -1 mV for GaAs. (b) Output currents I_{11} and I_{12} plotted over an applied source-drain voltage ranging from 0 to -7 mV for InAs.

and compute the current. We can see that in both materials, the vast majority of the current flows in the top waveguide (I_{11}) for small reverse biases. However, as we increase the reverse bias across the device, we see that the current ceases to flow in the top waveguide and transfers to the bottom waveguide (I_{12}). This occurs due to the fact that as the reverse bias is increased the top waveguide begins to pinch off as the Fermi energy at the end of the device has been lowered to such a degree that it becomes impossible for the top waveguide to sustain a propagating mode. Further, as the reverse bias increases, we are also modulating the velocity of the incoming mode. As the mode continues to slow, we see that the mode couples to the bottom waveguide as we have effectively changed the location of the coupling length that maximizes T_{12}. Moreover, as the mode continues to slow, we sweep through a highly reflective energy state which causes the null in the $I-V$ characteristics of each of the semiconductors. Finally, as the bias reaches its maximum, the Fermi energy at the output of the device reaches a level that is insufficient to sustain modes propagating in either the top or the bottom waveguide at the output of the device.

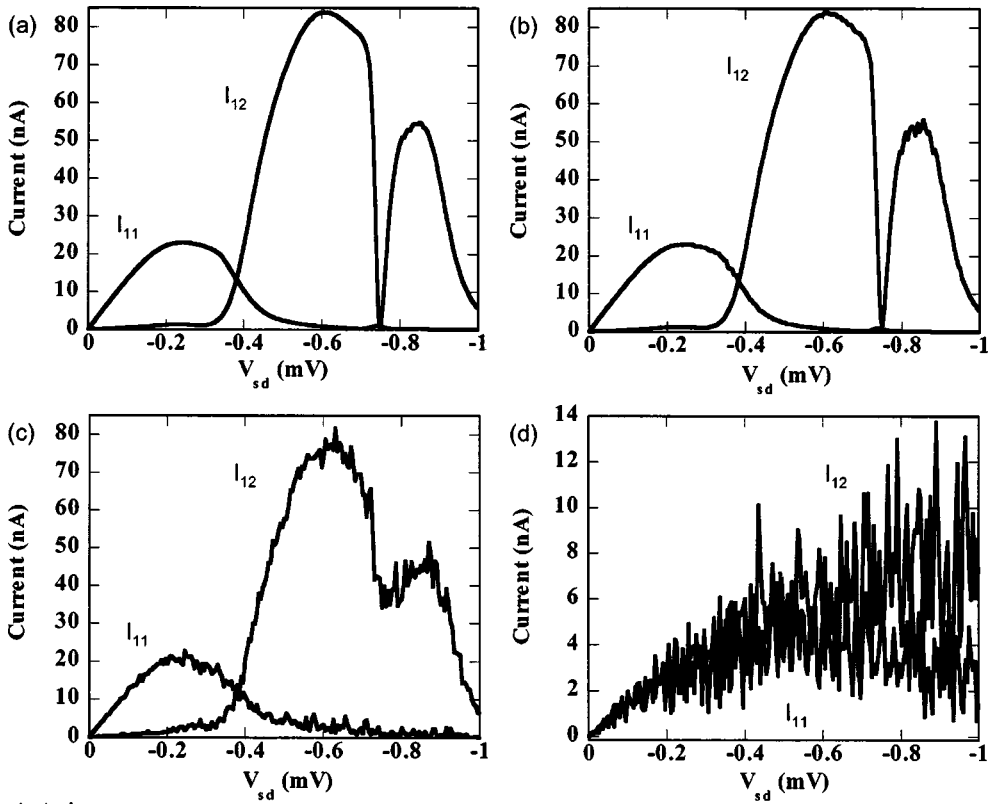

FIG. 4. (a) Output currents I_{11} and I_{12} plotted over an applied source-drain voltage ranging from 0 to -1 mV for GaAs with no disorder. (b) Output currents I_{11} and I_{12} plotted over an applied source-drain voltage ranging from 0 to -1 mV for GaAs assuming a mean-free path of 1×10^{-6} m. (c) Output currents I_{11} and I_{12} plotted over an applied source-drain voltage ranging from 0 to -1 mV for GaAs assuming a mean-free path of 1×10^{-8} m. (d) Output currents I_{11} and I_{12} plotted over an applied source-drain voltage ranging from 0 to -1 mV for GaAs assuming a mean-free path of 1×10^{-10} m.

Nevertheless, to examine the effects of disorder scattering on the ability of the semiconductor waveguide inverter's operation, we add a uniformly distributed random perturbation of energy width W to the on-site energy $E(i,j)$, which corresponds to a distribution of scatterers having a delta function potential, or

$$\frac{W}{E_F}=\sqrt{\frac{6\lambda_F^3}{\pi^3 a^2 \Gamma}}. \tag{1}$$

Here, λ_F is the Fermi wavelength, a is the grid spacing and Γ is the mean-free path.[5]

In Fig. 4, we examine the effects of disorder on the GaAs system. In Fig. 4(a), we see the normal $I-V$ characteristics of a GaAs waveguide inverter without the inclusion of disorder in the material. In Fig. 4(b), we assume a mean-free path of 1×10^{-6} m and see that the output characteristics do not really change significantly from the nondisordered characteristics. In Fig. 4(c), however, we see that for a mean-free path of 1×10^{-8} m the disorder introduced into the potential causes the null in the $I-V$ curves to be reduced. This is caused by the fact that the perturbation introduced in the potential forces the energy of the mode to be such that it never attains the critical value corresponding to the highly reflective energy value. Finally, in Fig. 4(d) we examine the $I-V$ characteristics corresponding to a mean-free path of 1×10^{-10} m. In the latter case, we see that it is no longer clear whether or not the mode will couple to the bottom waveguide. This occurs because the perturbations in the potential profile are significant enough to force the energy and, therefore, the velocity of the mode into random states where at one bias point the mode exists mainly in the top waveguide and then at the next bias point the mode resides mainly in the bottom waveguide. Therefore, an applied bias where we can be certain that the device has switched does not exist. Further, we also see a noticeable decrease in the output current of the device due to increased reflections from the sizable, random potential.

Similarly, in Fig. 5, we examine the role that disorder plays in the InAs inverter. In Fig. 5(a), we see the normal $I-V$ characteristics of an InAs waveguide inverter without the inclusion of disorder in the material. In Fig. 5(b), we assume a mean-free path of 1×10^{-6} m and see that the output characteristics do not really change significantly from the nondisordered characteristics, as seen in the GaAs system. In Fig. 5(c), however, we see that, for a mean-free path of 1×10^{-8} m, the disorder introduced into the potential causes the null in the $I-V$ curves to be reduced. This is caused by the fact that the perturbation introduced in the potential forces the energy of the mode to be such that it never attains the critical value corresponding to the highly reflective en-

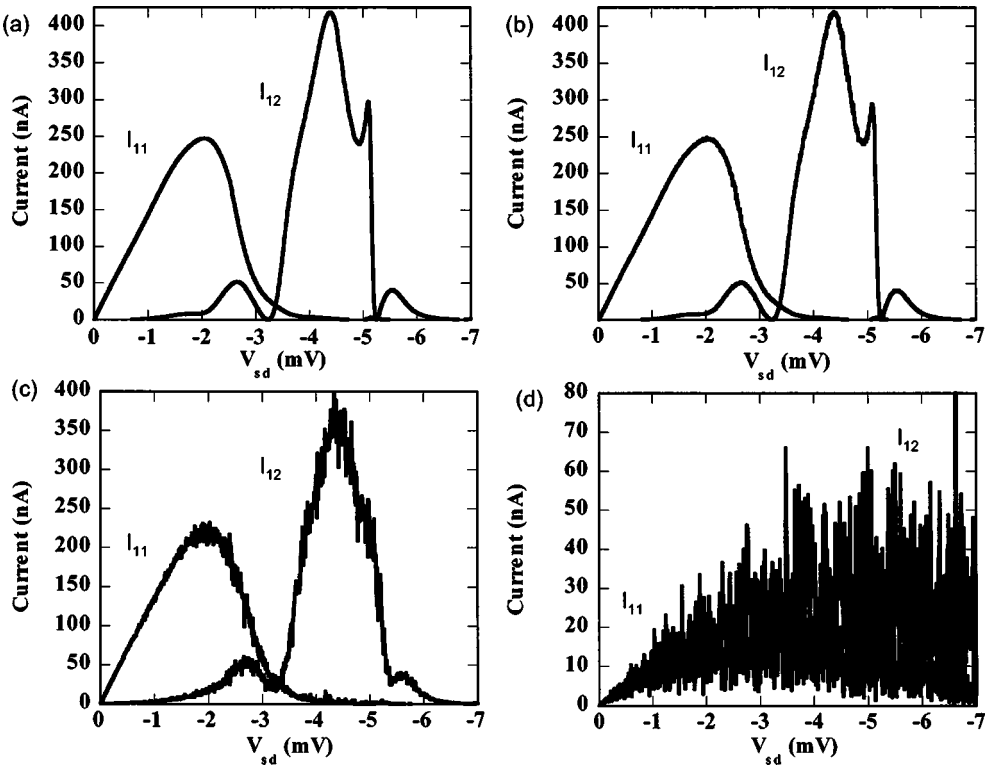

FIG. 5. (a) Output currents I_{11} and I_{12} plotted over an applied source-drain voltage ranging from 0 to -7 mV for InAs with no disorder. (b) Output currents I_{11} and I_{12} plotted over an applied source-drain voltage ranging from 0 to -7 mV for InAs assuming a mean-free path of 1×10^{-6} m. (c) Output currents I_{11} and I_{12} plotted over an applied source-drain voltage ranging from 0 to -7 mV for InAs assuming a mean-free path of 1×10^{-8} m. (d) Output currents I_{11} and I_{12} plotted over an applied source-drain voltage ranging from 0 to -7 mV for InAs assuming a mean-free path of 1×10^{-10} m.

ergy value. Finally, in Fig. 5(d) we examine the $I-V$ characteristics corresponding to a mean-free path of 1×10^{-10} m. In Fig. 5(d), just as in Fig. 4(d), we see that it is no longer clear whether or not the mode will couple to the bottom waveguide. Moreover, we also see the decrease in the output current due to increased reflections from the random potential. Therefore, we cannot be certain of proper device operation.

In summary, the operation of the coupled waveguide inverter seems to be stable under the presence of moderate disorder in the system for both the GaAs and the InAs systems. However, care must be taken when implementing this device in hetrostructures containing a significant amount of disorder as device operation is no longer predictable.

This work is supported by the Office of Naval Research.

[1]I. L. Chung and M. A. Nielsen, *Quantum Computing and Quantum Information* (Cambridge University Press, Cambridge, 2000).
[2]M. J. Gilbert, R. Akis, and D. K. Ferry, Appl. Phys. Lett. **81**, 4284 (2002).
[3]T. Usuki, M. Saito, M. Takatsu, R. A. Kiehl, and N. Yokoyama, Phys. Rev. B **52**, 8244 (1995).
[4]D. K. Ferry and M. A. S. M. Goodnick, *Transport in Nanostructures* (Cambridge University Press, Cambridge, 2000).
[5]T. Ando, Phys. Rev. B **44**, 8017 (1991).